doi:10.3788/gzxb20164510.1024001

# 基于 SPASER 机制的偏心金壳纳米天线的多波长散射特性

王勉[1]，张昊鹏[1]，许田[2]，周见红[3]，周骏[1]
(1 宁波大学 理学院,浙江 宁波 315211)
(2 南通大学 理学院,江苏 南通 226007)
(3 长春理工大学 光电子工程学院，长春 130022)

**摘 要**:基于表面等离激元受激辐射放大(SPASER)机制,提出了一种硅-金-硅三层核壳偏心纳米天线,并利用有限元法分析了其多波长散射特性.结果表明:在 SPASER 机制下,该纳米天线产生极大的散射光强度,且工作波长的数目随着硅核偏心率的增加而增加;当硅核的偏心率为 9 nm 时,该纳米天线有 4 个共振峰,分别位于 615 nm、656 nm、724 nm 、847 nm,其对应的散射强度比非 SPASER 机制的纳米天线的散射强度高 $10^4$ 倍;该纳米天线的散射波长还可以通过改变入射光的偏振角调节.基于 SPASER 机制的纳米天线对于设计多波长纳米激光器具有指导意义.

**关键词**:表面等离激元受激辐射放大;局域表面等离子体共振;吸收截面;散射截面;纳米天线
**中图分类号**:O433.4 **文献标识码**:A **文章编号**:1004-4213(2016)10-1024001-8

# Multi-wavelength Scattering Characteristics of a SPASER-based Off-centre Gold Shell Nanoantenna

WANG Mian[1], ZHANG Hao-peng[1], XU Tian[2], ZHOU Jian-hong[3], ZHOU Jun[1]
(1 *Faculty of Science, Ningbo University, Ningbo, Zhejiang* 315211, *China*)
(2 *School of Sciences, Nantong University, Nantong, Jiangsu* 226007, *China*)
(3 *School of Optoelectric Engineering, Changchun University of Science and Technology, Changchun* 130022, *China*)

**Abstract**: Based on the mechanism of the Surface Plasmon Amplification by Stimulated Emission of Radiation (SPASER), an off-centre gold shell nanoantenna consisted of the silica-gold-silica three-layer core-shell was proposed and its multi-wavelength light scattering characteristics were numerically analyzed by using the Finite Element Method (FEM). For the SPASER-based nanoantenna, the results show that, the scattering wavelength number increases with the increasing of the silica core eccentricity and the scattering light intensity is greatly enhanced. When the eccentricity of silica core is 9 nm, the proposed nanoantenna has four intensity resonance peaks which are located at 615 nm, 656 nm, 724 nm and 847 nm respectively, and the corresponded scattering intensities are much higher than that of the non-SPASER one, about $10^4$ times. Moreover, the scattering wavelengths of the proposed nanoantenna can be easily adjusted by changing the polarization angle of the incident light. The SPASER-based nanoantenna would be useful to design the multi-wavelength laser devices in nanoscale.

**Key words**: SPASER; Localized surface plasmon resonance; Absorption cross-sections; Scattering cross-

**Foundation item**: The National Natural Science Foundation of China (Nos. 61275153, 61320106014), the Open Fund of Key Subject of Physics, Zhejiang Province (Nos. xkzwl12, xkzwl1521), and the K. C. Wong Magna Fund of Ningbo University, China

**First author**: WANG Mian (1995—), female, B. S. degree candidate, mainly focuses on local surface plasmon of metal media/nano particle. Email:wangmianhh@126.com

**Corresponding author**: ZHOU Jun (1958—), male, professor, Ph. D. degree, mainly focuses on photonics, surface enhancement Raman spectrum and their applications in biosensing. Email:zhoujun@nbu.edu.cn

**Received**: Mar. 14, 2016; **Accepted**: Aug. 10, 2016

sections; Nanoantenna

**OCIS Codes**: 240.6680; 160.4236; 250.5403; 290.4210

# 0 Introduction

The plasmonic metallic nanosystems have been paid a great attention to focus on their abilities of strongly scattering light for far-field and intensely inducing the local electric field enhancement[1-5]. And the optical properties of the plasmonic metallic nanosystems are able to tailor by changing their structure such as size, configuration, morphology and components[6-8]. Specially, the generation of a high-strength scattering field is the key to realize an optical nanoantenna based on the Localizsed Surface Plasmon Resonance (LSPR)[9-14]. A typical metallic nanoantenna, the non-centrosymmetry layered noble nanoantenna has recently attracted more interests due to its distinct characteristics. Hu's group found that the operate wavelength and the scattering strength of the gold-silica-gold nanoantenna can be controlled by designing of its geometric structure because of the hybridization of the multipolar plasmon modes[15]. Mukherjee's group demonstrated that the non-centrosymmetry gold-silica-gold nanoantenna can built a fano resonance due to the overlapping energy between the superradiant plasmon mode and the subradiant plasmon mode[16]. However, the scattering intensity of these plasmonic metallic nanosystems cannot be enormously improved by only adjusting their geometric parameters. Fortunately, by introducing the mechanism of the Surface Plasmon Amplification by Stimulated Emission of Radiation (SPASER), the plasmonic mode and the scattering intensity of metallic nanosystem can be dramatically amplified to make it to be an efficient nanoantenna[17]. The physical insight of the SPASER can be described essentially as the Surface Plasmon (SP) amplification process in which the propagation loss of SP of the noble metal nanosystem is completely compensated by transferring the exciting energy of gain materials to the metal under an exciting irradiation[18-22]. Naturally, it is necessary that the SPASER system should possess three elements: The noble metal nanostructure to produce LSPR, the suitable gain materials to produce energy gain, and the exciting energy of gain materials to compensate the energy loss of LSPR modes in the noble metal nanostructure. Therefore, the SPASER-based metallic nanostructure is adequate to fulfill the demands of high-performance optical nanoantenna.

In this work, the SPASER-based off-centre nanosystem consisted of silica-gold-silica three-layer core-shell structure was proposed and its great ability of far-field scattering light was demonstrated. Results show that, the multipolar plasmon modes of the proposed nanoantenna can be turned in the range of visible wavelength, the modulation can be achieved by two ways; First, adjusting the off-centre of silica core in gold shell, second, adjusting the polarization angle of incident light. It exhibits an excellent performance of plasmonic nanoantenna for a greater range of various off-center degrees and polarization lights.

# 1 Model and theory

As shown in Fig. 1, the configuration of the SPASER-based off-centre nanoantenna includes a silica core diverged from the geometric centre of nanoantenna and a gold shell encapsulated by an outer silica shell. And the silica core and the silica shell are doped a same gain material. The radii of the silica core, the gold shell and the outer silica shell are $R_1$, $R_2$ and $R_3$, respectively. The eccentricity of the silica core is denoted as $\Delta$ to describe the distance between the center of silica core and the geometric center of nanoantenna. For simplicity, the refractive indices of the silica core and outer silica shell are set as $n_{\text{silica}}=1.5-\mathrm{j}(k_1+k_2+k_3+\cdots+k_n)$, where $k_1, k_2, k_3, \cdots, k_n$ are the optical loss/gain coefficients at different wavelengths which describe the dissipation/amplification of the incident light in the silica media with gain material[18,21]. The dielectric constant of gold is obtained from the experimental data of Johnson and Christy[23]. The SPASER-based off-centre gold shell nanoantenna is surrounded by the air with refractive index $n_0=1.0$. And the incident light propagates along the $x$-axis and its polarization direction is paralleled to the $z$-axis.

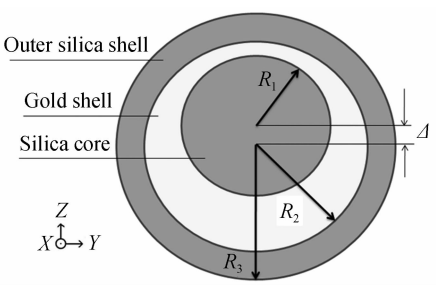


Fig. 1 Configuration of the nanoantenna with an off-centre silica-gold-silica core-shell

According to Mie theory, the scattering and absorption properties of the SPASER-based off-centre gold shell nanoantenna are analyzed in the frequency domain by using the scattering field formulation. The scattering cross-section $C_{\text{scat}}$ is integrated by the normalized electric field around a far-field transform

boundary enclosing the whole system and expressed as follow[6]

$$C_{\text{scat}} = \frac{1}{\boldsymbol{E}_{\text{inc}}^2}\int |\boldsymbol{E}_{\text{far}}|^2 \mathrm{d}S \tag{1}$$

where $\boldsymbol{E}_{\text{far}}$ is the far-field electric component of the scattering field calculated by the Stratton-Chu formula[24] and $\boldsymbol{E}_{\text{inc}}$ is the incident electric field amplitude. Absorption cross-section $C_{\text{abs}}$ is obtained by integrating the time-average resistive heating ($U_{\text{av}}$)[25]

$$C_{\text{abs}} = \frac{2}{\sqrt{\varepsilon_0/\mu_0}\,\boldsymbol{E}_{\text{inc}}^2}\int U_{\text{av}}\mathrm{d}V \tag{2}$$

where $\varepsilon_0$ and $\mu_0$ are permittivity and permeability of vacuum, respectively. And, $U_{\text{av}} = \frac{1}{2}\mathrm{Re}(\sigma\boldsymbol{E}\cdot\boldsymbol{E}^* - \mathrm{j}\omega\boldsymbol{E}\cdot\boldsymbol{D}^*)$, $\sigma$ is the conductivity of the integrated material, $\omega$, $\boldsymbol{E}$ and $\boldsymbol{D}$ are angular frequency, electric field vector and electric displacement vector of the incident light, respectively.

As a precision and effective numeric calculation method of the electric field distribution, the Finite Element Method (FEM) is generally used to analyze the optical characteristics of metallic nanostructures by solving the time-harmonic Maxwell equations on an adaptive discretized spatial grid[26]. In our works, the $C_{\text{abs}}$ and $C_{\text{scat}}$ spectra of the SPASER-based off-centre gold shell nanoantenna are obtained by using a commercial FEM package (COMSOL Mutiphysics 4.3 with RF module). To avoid the nonphysical reflections of emergent electromagnetic waves from the grid boundaries, the perfectly matched layers of absorbing boundaries are used around the nanoantenna.

## 2 Results and discussion

We firstly consider the case of non-SPASER nanoantenna with $R_1 = 30$ nm, $R_2 = 40$ nm, $R_3 = 50$ nm, $n_{\text{silica}} = 1.5$ and $k_i = 0$ ($i = 1, 2, 3, \cdots, n$). The absorption cross-sections spectra of the SPASER-based nanoantenna are calculated and show in Fig. 2(a). As well known, LSPR modes of plasmonic metallic nanostructure are originated from the oscillations of the free electrons on the metal surface of the metallic nanostructure under the excitation of the external irradiation field[10]. And, the different wave vector of incident light will induce the different absorption cross-sections of plasmonic metallic nanostructure[27]. Here, the peaks of absorption cross-sections spectra in Fig. 2 (a) are corresponding to the LSPR modes of the off-centre gold shell nanostructure. Thus, we can see that the number of LSPR modes in Fig. 2(a) increases along with the increasing of the eccentricity of silica core $\Delta$. For example, corresponding to $\Delta = 0$, 4, 8 and 9 nm, the absorption peaks are increased from one peak to four peaks . In other words , the number of LSPR

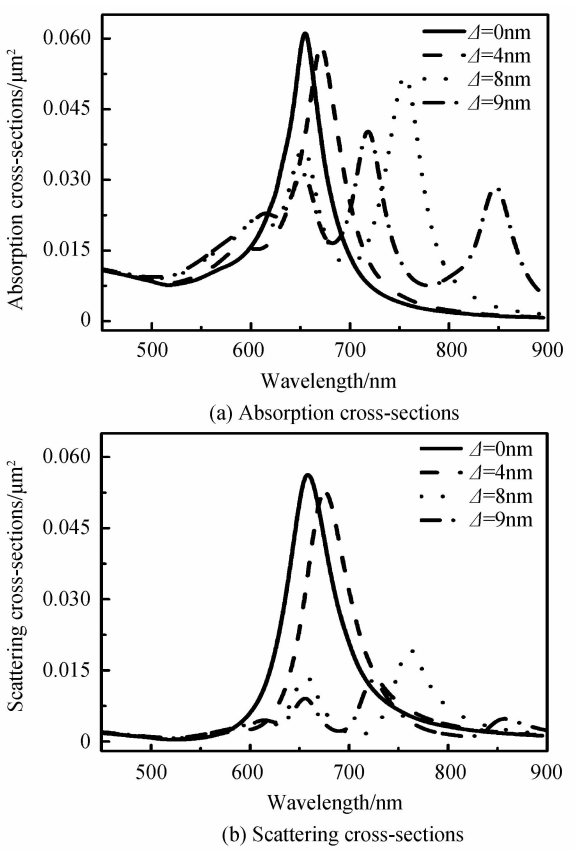


Fig. 2 Optical cross-sections spectra of the off-centre core-shell nanostructure with the different eccentricity of core $\Delta$

modes can be easily controlled by the changing of structure symmetry, which means the operate wavelengths of the off-centre gold shell nanoantenna are able to be tailored and the positions of the LSPR peaks red shift as well. As shown in Fig. 2(b), when $\Delta = 9$ nm, the four scattering peaks are located at 615, 656, 724 and 847 nm, respectively, and the LSPR dipole mode red-shifts to 847 nm from original 660 nm at $\Delta = 0$. It can be explained by plasmon hybridization mode[10, 15]. As show in Fig. 3, the plasmon shell-modes of the gold nanoshell, such as bonding mode and anti-bonding mode, are originated from the interaction of the core-modes of gold core and the cavity-mode of gold cavity, and the mode of a centrosymmetry gold shell nanostructure is forbidden. By increasing the eccentricity of silica core, the selection rules of interaction are relaxed, allowing the different orders modes to be mutually coupled, so that the other three multipolar modes can be generated in the spectrum when $\Delta = 9$ nm. Thus the interactions between the core modes and the cavity modes became weaker as the increasing of the eccentricity of the silica core, which results in the red-shifts of LSPR peaks and the decrease of the peak values of absorption/scattering cross-sections as the increasing of $\Delta$. Meanwhile, the absorption cross-sections of the SPASER-based

nanoantenna is positive, which means the energy of the incident light is consumed and the energy loss of the off-centre gold shell nanostructure cannot be efficiently compensated. Therefore, the off-centre gold shell nanostructure cannot be used as a nanoantenna yet.

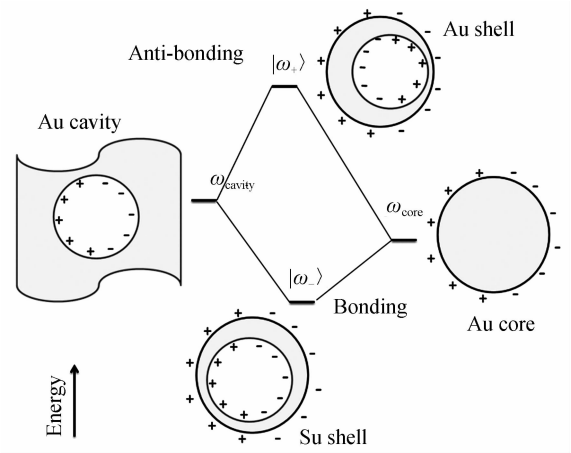


Fig. 3 Plasmon hybridization diagram of the gold shell structure

Subsequently, the optical spectra of the SPASER-based off-centre gold shell nanoantenna are calculated with the above same parameters and show in Fig. 4. It is obviously different from that of the above non-SPASER one. Comparing Fig. 4 with Fig. 2(b), the scattering cross-sections of SPASER-based nanoantenna at 615, 656, 724 and 847 nm are drastically increased to $2.5\times10^4$, $3.1\times10^4$, $1.8\times10^4$ and $1.7\times10^4$ times of the non-SPASER one, respectively. In the other words, the LSPR mode of the SPASER-based nanoantenna is greatly amplified by the introducing of SPASER mechanism. And we can see from Fig. 4, the linewidths of optical cross-sections are much narrow and the absorption cross-sections are negative, which means the SPASER-based nanoantenna does not dissipate energy but compensate the energy losses of the LSPR modes. It is worth to note that the amplifications of optical cross-sections at different work wavelengths need to be compensated by different optical gain, respectively. It is to say that,

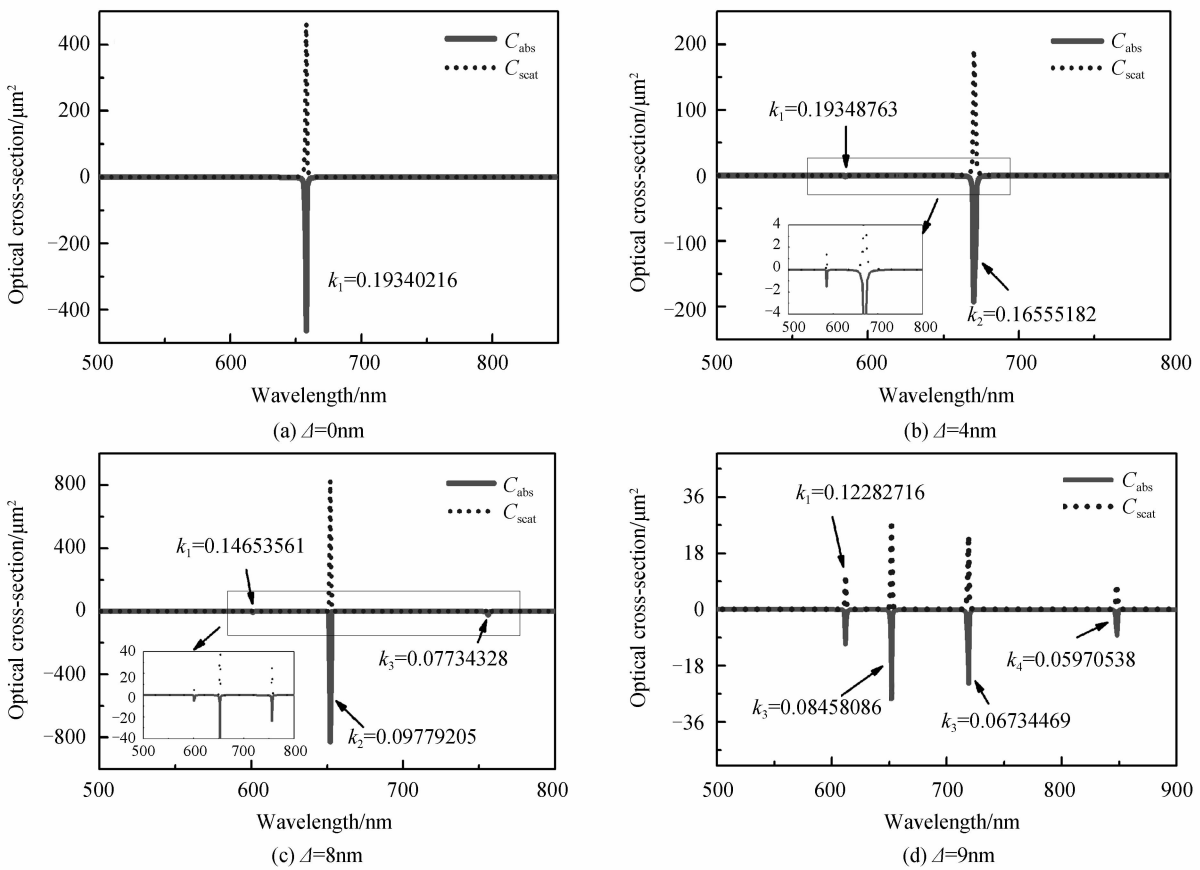


Fig. 4 Optical cross-section spectra of the SPASER-based nanoantenna with different eccentricity of core

the $k$ values of the doped gain materials in silica should be chosen by matching the values of optical cross-sections to satisfy $C_{abs} + C_{scat} = 0$ for the different exciting wavelength. At same time, the dichotomy is used to correct the shifting of work wavelength induced by $k$. Taking the example of the SPASER-based nanoantenna with $\Delta = 9$ nm, four kinds of gain materials at the exciting wavelengths of 615, 656, 724 and 847 nm should be doped in silica simultaneously, which correspond to the optical gain coefficient $k =$ 0.122 827 16, 0.084 580 86, 0.067 344 69 and 0.059 705 38, respectively. It implies that the doped

amount of gain material in silica is also different for effectively implementing the performance of SPASER-based nanoantenna.

Furthermore, at the exciting wavelength of 847 nm, the optical cross-sections spectra of the SPASER-based nanoantenna with $\Delta = 9$ nm are calculated for the different gain coefficients $k$ and shown in Fig. 5. It is clearly that $C_{abs}$ and $C_{scat}$ change sensitively with $k$. As we can see, when $k=0$, the peaks of $C_{abs}$ and $C_{scat}$ are both centered at 847nm with a linewidth of 48 nm, and the value of $C_{abs}$ is much larger than that of $C_{scat}$, which means the energy from the exciting light is consumed due to the LSPR of the gold nanoshell. However, when $k=0.056\ 25$ (Fig. 5 (b)), the scattering is greatly enhanced with a narrow linewidths of 10 nm and the absorption is negative. It should be pointed that, Fig. 5 (c) shows a stable operation of the SPASER-based nanoantenna at the critical point of $k=0.059\ 705\ 38$, where the values of $C_{abs}$ and $C_{scat}$ are 8.260 1 $\mu m^2$ and $-8.260\ 1$ $\mu m^2$, respectively. Comparing Fig. 5 (c) with Fig. 5(a), the values of $C_{abs}$ and $C_{scat}$ are increased by three orders of magnitudes and the linewidths of peaks abruptly decrease to about 0.5 nm due to the doping gain material in silica. If the value of $k$ continuously grows, as we can see in Fig. 5 (d), the absolute value of $C_{abs}$ and $C_{scat}$ decrease and their linewidths increase. Therefore, it is reasonable to regard $k=0.059\ 705\ 38$ as the "threshold" for building up such strong surface plasmon amplification. Besides, at wavelengths of 615, 656 and 724 nm, when the gain coefficients $k$ are 0.122 827 16, 0.084 580 86 and 0.067 344 69, the corresponded scattering intensities are $2.5\times10^4$, $3.1\times10^4$, $1.8\times10^4$ times of the non-SPASER one, respectively. Therefore, it also suggests that the scattering of the SPASER-based gold shell nanoantenna is dependent on the gain materials and much higher than that of the non-SPASER one at all operate wavelengths.

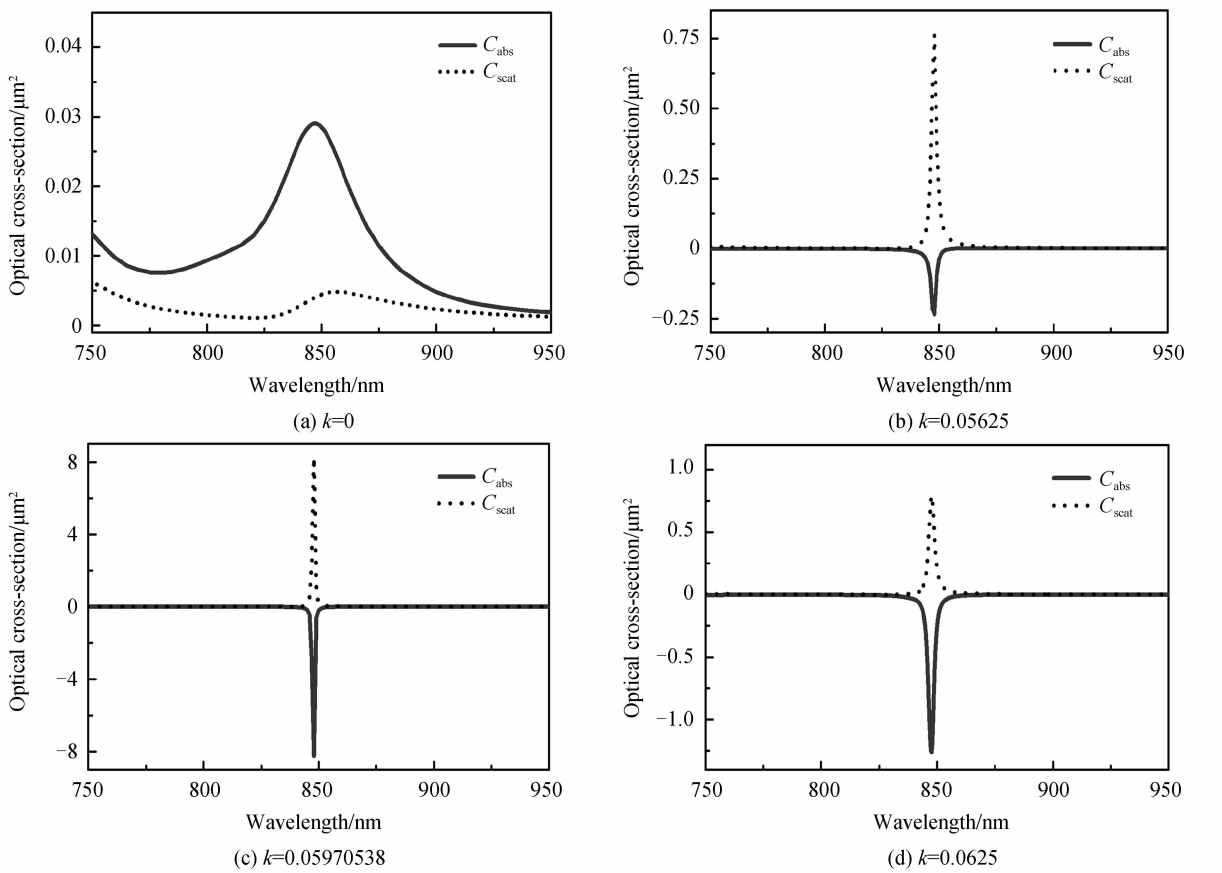


Fig. 5 Optical cross-sections spectra of the SPASER-based nanoantenna with the eccentricity of $\Delta=9$ nm for different $k$

Based on the SPASER mechanism, the enhanced scattering is easily understand because of the SP amplification raised from the interactions among the gain material doped in silica, gold nanoshell and the incident light[16, 18-20]. In fact, these interactions are a dynamic process: The gain material is excited to provide energy compensating the loss of LSPR mode in the gold nanoshell and form the SP amplification, in return, the LSPR mode regulating photons in the doped silica by a means of strength-related feedback. When $k$ is below threshold, after the excited energy of gain material is not enough to compensate the loss of LSPR

mode in the gold nanoshell, but absorbs the energy of incident light. When $k$ reaches the threshold, the energy absorbed by the gain material is completely transferred to the LSPR modes by energy resonance so that the SP amplification is realized by dynamic photo-plasmon coupling between the gold nanoshell and the incident light. Finally, a super-resonance holds and the net amplification is zero, whereas the resonance linewidth diminishes. When $k$ exceeds the thresholds, the stable operate condition of SPASER is crashed and the SP amplification vanishes. The above process can be intuitively illustrated by the distribution of local field intensities of the proposed SPASER-based nanoantenna. As shown in Fig. 6(a), while $k=0$, the

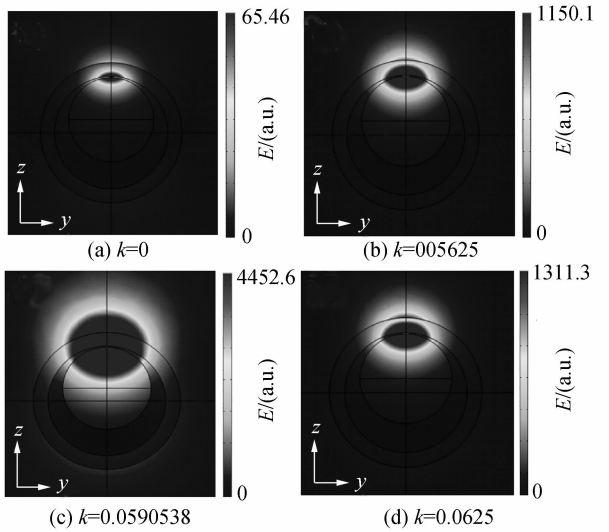


Fig. 6 Electric field distribution ($yz$-plane) of the SPASER-based nanoantenna with $\Delta=9$ nm for different $k$

electric field is very weak. With the increasing of $k$ (Fig. 6(b)), the intensities of electric field become stronger, but excited energy is still not high enough to realize super-resonance. With more gian material added into the nanoatenna, at the point of $k=k_{\text{threshold}}$ (Fig. 6(c)), the intensities of electric field reached a pretty high value, the SP amplification is realized and a super-resonance holds. While $k$ continues to be increased and exceeds the thresholds (Fig. 6(d)), the intensities of electric field become weak again and the SP amplification vanishes.

In addition, the spectral response of the SPASER-based nanoantenna dependent on the polarization angles of incident light is shown in Fig. 7. Comparing Fig. 7(a) with Fig. 7(b), in the case of polarization angle 30°, the absolute values of $C_{\text{abs}}$ and $C_{\text{scat}}$ dramatically and a new peak at 709 nm arises along with a slight blue shift. Actually, the new peak is already exists in the spectrum of polarization angle 0° but too small to distinguish easily, as shown in insert of Fig. 7(a). The strong peak is necessary because the establishment of SPASER behavior needs an energy resonance transfer between gain material and gold nanoshell to effectively compensate the energy loss of plasmon mode of the gold nanoshell and form the SP amplification. However, if the compensating energy generated by doped gain material is more or less than the energy loss, the SPASER mechanism will not be efficient[18-20]. Thus, $k$ was calculated to be 0.067 344 69 which efficiently generated the SPASER behavior in 709 nm when the polarization angle is 30°. Complementary, the blue shift of the low order peaks is more obvious than that of high order peaks due to the inefficient SPASER mechanism, which is in agreement with the plasmon hybiridization theory[10, 15]. When the polarization angle is 60°, as shown in Fig. 7(c), the peaks in the spectrum continually blue shift and their strength are continually decreased. Although the strength of scattering peaks is dropped, they are still greater about two orders of magnitude than that of the non-SPASER one. When the polarization angle of the incident light is 90°, however, the dipolar mode vanishes because the LSPR dipolar mode of the off-central gold shell cannot be excited so that the efficient amplification of the LSPR absents, in other words, the

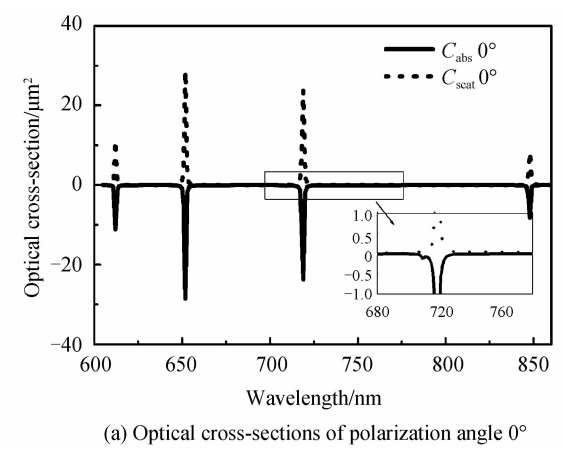


(a) Optical cross-sections of polarization angle 0°

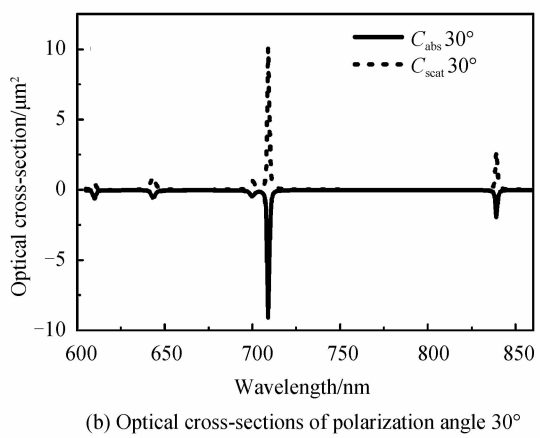


(b) Optical cross-sections of polarization angle 30°

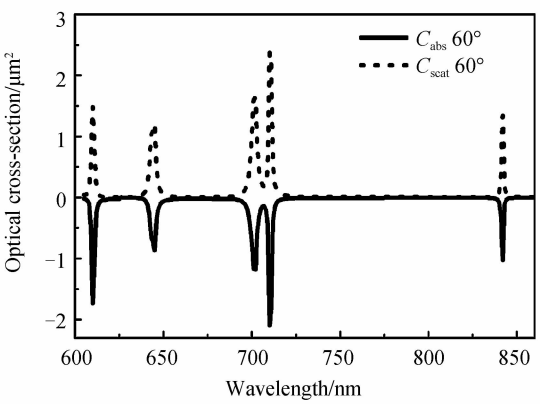


(c) Optical cross-sections of polarization angle 60°

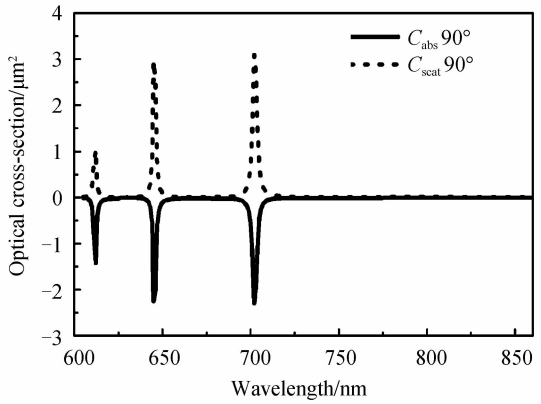


(d) Optical cross-sections of polarization angle 90°

Fig. 7 Optical cross-section spectra of the SPASER-based nanoantenna at $k=0.067\ 344\ 69$ for the incident light along with the $z$-axis

SPASER mechanism is inapplicable. It is worth pointed that SPASER mechanism can efficient act on the other wavelengths to make the SPASER-based nanoantenna is still a multi-wavelength optical nanoantenna at this moment.

And more, as we can see, each peak in the spectra is easily to be distinguished, which means their strength and the linewidth are suitable as a multi-wavelength nanoantenna. Without any adjustment of geometries, the output wavelength of SPASER-based nanoantenna can be manipulated by only changing the polarization angle of the incident light, which provides us an easy method to modulate the output performance of SPASER-based nanoantenna. It is important for designing and fabricating of a low-cost and high quality SPASER-based nanoantenna. Moreover, if the SPASER-based layered core-shell nanoantenna is simultaneously excited by the incident light beams with different polarization angles, the response of the optical cross-section spectra is similar to the light extraction effect[28]. That is, the principle of SPASER-based nanoantenna may be applied to design optical nano-filter by amplifing the specific output wavelength.

## 3 Conclusion

In summary, the SPASER-based off-centre silica-gold-silica has been theoretically proposed as a multi-wavelength nanoantenna due to the enormously increase of scattering cross-section. We found that by introducing SPASER mechanism, the scattering cross-section of the SPASER-based layered core-shell nanoantenna at 615, 656, 724 and 847nm are $2.5\times10^4$, $3.1\times10^4$, $1.8\times10^4$ and $1.7\times10^4$ times of the no SPASER one, respectively. Besides, at the threshold point of gian material $k_{\text{threshold}}$, the intensities of electric field exhibit a enormously enhancement and the SP amplification is realized. Excepting a great amplification of the scattering cross-section, the operate wavelength of the SPASER-based layered core-shell nanoantenna is controllable by only changing the polarization angle of the incident light. Therefore, the proposed SPASER-based nanoantenna is useful for designing a passive optical nanoantenna with high performance and other optical functional devices.

**References**

[1] PRODAN E, RADLOFF C, HALAS N J, *et al*. A hybridization model for the plasmon response of complex nanostructures[J]. *Science*, 2003, **302**(5644): 419-422.

[2] KING N S, Li Y, AYALA-OROZCO C, *et al*. Angle and spectral-dependent light scattering from plasmonic nanocups [J]. *ACS Nano*, 2011, **5**(9): 7254-7262.

[3] KINIGHT M W, HALAS N J. Nanoshells to nanoeggs to nanocups: optical properties of reduced symmetry core - shell nanoparticles beyond the quasistatic limit[J]. *New Journal of Physics*, 2008, **10**(10): 105006.

[4] MING Tian, ZHAO Lei, YANG Zhi, *et al*. Strong polarization dependence of plasmon-enhanced fluorescence on single gold nanorods[J]. *Nano Letters*, 2009, **9**(11): 3896-3903.

[5] WU D J, LIU X J. Optimization of silica-silver-gold layered nanoshell for large near-field enhancement [J]. *Applied Physics Letters*, 2010, **96**: 151912.

[6] ZHANG Li, ZHOU Jun, JIANG Tao. Gain-assisted U-shaped Au nanostructure for ultrahigh sensitivity single molecule detection by surface-enhanced Raman scattering[J]. *Journal of Optics*, 2015, **17**: 125003.

[7] YUAN Yu-yang, YUAN Zong-heng, LI Xiao-nan, *et al*. Absorption enhancement and sensing properties of Ag diamond nanoantenna arrays[J]. *Chinese Physics B*, 2015, **7**(24): 074206.

[8] DENG Hu, CHEN Qi, HE Xiao-yang, *et al*. Power combining technology in three-way Terahertz photoconductive antenna[J]. *Chinese Journal of Luminescence*, 2014, **35**(12): 1500-1505.

[9] LIU Sen-bo, FU Hao, LI Xiao-long, *et al*. Characteristics of polymer waveguide sensor based on local surface plasmon resonace[J]. *Chinese Journal of Luminescence*, 2016, **37**(1): 112-116.

[10] MIGUEL N C, MAIER S A. Broad-band near-infrared plasmonic nanoantennas for higher harmonic generation[J]. *ACS Nano*, 2012, **6**(4): 3537-3544.

[11] DEVILEZ A, BRIAN S, NICOLAS B. Compact metallo-

dielectric optical antenna for ultra directional and enhanced radiative emission[J]. *ACS Nano*, 2010, **4**(6): 3390-3396.

[12] HATAL N A, HUSUEH C H, GADDIS A L, *et al*. Free-standing optical gold bowtie nanoantenna with variable gap size for enhanced Raman spectroscopy[J]. *Nano Letters*, 2010, **10**(12): 4952-4955.

[13] PAKIZEH T, MIKAEL K. Unidirectional ultracompact optical nanoantennas[J]. *Nano Letters*, 2009, **9**(6): 2343-2349.

[14] AOUANI H, MAHBOUB O, DEVAUX E, *et al*. Plasmonic antennas for directional sorting of fluorescence emission[J]. *Nano Letters*, 2011, **11**(6): 2400-2406.

[15] HU Ying, NOELCK S J, DREZEK R A. Symmetry breaking in gold-silica-gold multilayer nanoshells[J]. *ACS Nano*, 2010, **4**(3): 1521-1528.

[16] MUKHERJEE S, SOBHANI H, LASSITER J B, *et al*. Fanoshells: nanoparticles with built-in Fano resonances[J]. *Nano Letters*, 2010, **10**(7): 2694-2701.

[17] BERGMAN D J, STOCKAMN M I. Surface plasmon amplification by stimulated emission of radiation: quantum generation of coherent surface plasmons in nanosystems[J]. *Physical Review Letters*, 2003, **90**: 027402.

[18] GORDON J A, ZIOLKOWSKI R W. The design and simulated performance of a coated nano-particle laser[J]. *Optics Express*, 2007, **15**(5): 2622-2653.

[19] LI Zhi-yuan, XIA You-nan, *et al*. Metal nanoparticles with gain toward single-molecule detection by surface-enhanced Raman scattering[J]. *Nano Letters*, 2010, **10**(1): 243-249.

[20] LIU Si-yun, LI Jia-fang, ZHOU Fei, *et al*. Efficient surface plasmon amplification from gain-assisted gold nanorods[J]. *Optics Letters*, 2011, **36**(7): 1296-1298.

[21] ZHANG Hao-peng, ZHOU Jun, ZOU Wei-bo, *et al*. Surface plasmon amplification characteristics of an active three-layer nanoshell-based SPASER[J]. *Journal of Applied Physics*, 2012, **112**: 074309.

[22] DING Pei, HE Jin-na, Wang Jun-qiao, *et al*. Low-threshold surface plasmon amplification from a gain-assisted core - shell nanoparticle with broken symmetry[J]. *Journal of Optics*, 2013, **15**: 105001

[23] JOHNSON P B, CHRISTY R W. Optical constants of the noble metals[J]. *Physical Review B*, 1972, **6**(12): 4370.

[24] FANG Yu-rui, LI Zhi-peng, HUANG Ying-zhou, *et al*. Branched silver nanowires as controllable plasmon routers[J]. *Nano Letters*, 2010, **10**(5): 1950-1954.

[25] HARADA Y, ASAKURA T. Radiation forces on a dielectric sphere in the Rayleigh scattering regime[J]. *Optics Communications*, 1996, **124**(5): 529-541.

[26] AOUANI H, RAHMANI M, ŠÍPOVÁ H, *et al*. Plasmonic nanoantennas for multispectral surface-enhanced spectroscopies[J]. *Physical Chemistry C*, 2013, **117**(36): 18620-18626.

[27] PELTON M, BRYANT G W. Introduction to metal-nanoparticle plasmonics[M]. John Wiley & Sons, 2013.

[28] PELLEGRINI G, MATTEI G, MAZZOLDI P. Light extraction with dielectric nanoantenna arrays[J]. *ACS Nano*, 2009, **3**(9): 2715-2721.